



Update of the Reference Ice Thickness Amounts due to Freezing Rain for Canadian Codes and Standards

Philip Jarrett¹, Ka-Hing Yau¹, Robert Morris¹

¹ *Engineering Climate Services Unit, Environment and Climate Change Canada, Toronto, Canada*

philip.jarrett@canada.ca, kahing.yau@canada.ca, robert.morris@canada.ca

Abstract— Ice accretion due to freezing rain is a hazard to society in many ways. Extreme icing events, in particular, can cause structural failure of electrical energy distribution systems and result in power outages affecting thousands of individuals, sometimes for a week or longer. Canadian standards for electrical transmission lines, telecommunication towers and highway bridges provide reference ice amounts for structural design such as the 50-year equivalent ice thickness on a transmission line conductor. The approach to calculating these design values involve applying an ice accretion model at long-term 24/7 staffed weather stations with standard meteorological hourly observations such as precipitation amounts, wind speed and present weather codes to indicate the occurrence of freezing precipitation. This paper describes an update to this data at about 200 Canadian weather stations based on the period from 1953 to 2018. The previous update was conducted in 2009 using observations up to 2007. This paper describes evolving issues with meteorological instruments and observing practices. The ice accretion models used will be described (Châiné, Goodwin, CRREL simple model). The extreme value distributions and fitting methods used in this project to calculate the 50-year return levels are also described and compared.

Keywords—ice accretion, freezing rain, ice loads, transmission lines, extreme value analysis

I. INTRODUCTION

Freezing rain is a significant cold season hazard for many parts of Canada. Even small amounts often result in traffic accidents and pedestrian injuries due to slippery, ice-covered roads and other surfaces. Freezing rain is also a hazard to aviation. Ice accretion on structures imposes loads that, in general, need to be accounted for in their design to avoid or minimize damage due to the weight of ice alone or in combination with wind loads that can occur during or following freezing rain events.

Canadian design standards for electrical transmission lines, telecommunication towers and highway bridges (e.g. [1], [2], [3], and [4]) account for ice loads due to freezing rain. The purpose of this work is to update ice accretion amounts that will be available for incorporation into these and other Canadian standards, as appropriate. Note that only freezing precipitation is considered, not other forms of ice accretion such as in-cloud rime icing or frozen wet snow.

II. ESTIMATING ICE ACCRETION AMOUNTS

Since there are no Canada-wide network observations of ice accretion due to freezing rain, the most available long-term data sets used in freezing rain studies correspond to standard hourly weather observations at 24/7 staffed weather stations generally at airports. The occurrence of weather including precipitation type and an indication of intensity (light, moderate or heavy) is observed and recorded each hour. These observations are generally referred to as ‘present weather’.

The actual ice accumulation on a structure, surface or object is not routinely observed and recorded at weather stations, but can be estimated for each hour by ice accretion models using the hourly ‘present weather’ codes along with daily total precipitation amounts to estimate hourly freezing rain amounts. The following list describes the steps in the data processing and analysis.

- **Data Extraction.** The required hourly and daily observations for the identified locations are extracted from the Environment and Climate Change Canada (ECCC) archived data files and compiled into time series files.
- **Station Joining.** Many stations end and another starts at the same time at the same or very close location with a different climate ID. Those cases are identified and the stations are joined to have a single, longer record. The climate ID of the most recent station is used for the entire record. (There were 215 locations with at least 10 years of data used for further analysis after this processing step.)
- **Substitute Co-located Precipitation Data.** In a few cases, at the 24/7 staffed stations, observations of daily precipitation end. If there are ECCC co-located autostations with daily precipitation from all-season weighing gauges these daily records are added to the staffed station’s record for the years with absent daily precipitation. The weighing gauge data is also adjusted to account for known low bias.
- **Estimating Hourly Precipitation.** The time series files with daily precipitation are processed to estimate the hourly freezing, frozen and liquid precipitation amounts. Freezing precipitation amounts are estimated for the hours with either freezing rain or freezing drizzle in that hour’s present weather observations.
- **Winter Year and Data Completeness.** Since icing events are analysed based on a winter year (e.g. the period corresponding to winter year 2006 is August 1, 2005 to July 2006), the time series files are trimmed to start August first of the first year in the file and end no later than July 31 of the last year. An inventory of the count of daily and hourly observations for the cold season of each winter year is compiled for later use in determining data completeness.
- **Identify Icing Events.** Unique icing events are compiled at each location and written to an icing events file. An event starts with the first occurrence of freezing precipitation. The event continues with each subsequent hour added until the temperature rises above 1°C or until there are no further occurrences of freezing rain for 72 consecutive hours. The data record for each hour in the event includes an assigned event ID, date-time, temperature, dew point, wind speed and direction and the freezing precipitation amount.
- **Ice Accretion Models.** The ice accretion amounts are calculated next and compiled in a separate file. For each hour,

the elements of the icing event are recorded in addition to the results of the ice accretion models for that hour including the incremental and accumulated amounts of ice on a horizontal surface, on a vertical surface, and the radial thickness from each of three models (Châiné, Goodwin and CRREL), the estimated maximum 10-minute average wind speed, and transverse load.

- **Icing Event Summary Data.** For each event, a single record is written including the event ID, date-time, maximum and minimum temperatures and wind speed, total accumulated ice on vertical and horizontal surfaces, the radial ice thickness from each of the 3 models, the estimated maximum 10-minute average speed and transverse load, and the winter year.

- **AMS (annual maximum series).** For each element of interest, an AMS is compiled listing the maximum value of the selected element for each winter year, and the number of events that occurred in each year. The data inventory compiled is used so that if there are no icing events for a winter year, and the cold season for the winter year is sufficiently complete, then that winter year's maximum is recorded as a zero, so that non-icing years are accounted for in the extreme value analysis at the next step. Elements for which AMS data are compiled include the Châiné radial thickness, and amounts on horizontal and vertical surfaces.

- **EVA (extreme value analysis).** For each of the AMS fields compiled, a series of extreme value analyses are performed. The Gumbel distribution is fitted by each of three methods: method of moments, method of L-moments and generalized least squares. The GEV (Generalized Extreme Value) distribution is also fitted by L-moments. The number of complete non-icing years, are considered a separate population and are accounted for in calculating the 50-year return level values. Outputs are compiled in a single file with a record for each location summarizing that location's results. Also, a PDF file is generated for each location with a graph of the AMS values and the fitted distributions and their 50-year return level results.

A. ECCC Archived Observations

The climatological database used in this project comprises data starting in 1953 for the earliest stations. Data up to July 2018 was used, where available. For locations such as major airports with complete data starting in 1953 and ending in 2018, the period of record is 65 years (winter years from 1954-2018).

The major issue related to station joining concerns the change in long-term observing practices at major airports. Until the early to mid-2010's, staffed airport weather stations used ECCC-supplied instruments and data collection and reporting systems. In the last decade almost all airport staffed weather stations have changed to a commercial reporting system acquired and managed by Nav Canada. For the most part, observations are similar, but come into the ECCC data systems and are archived in a different manner. When the change occurred, new climate IDs and names were assigned to the new Nav Canada stations in the ECCC data systems. For instance, Yellowknife A 2204100 operated since 1953 and changed to Yellowknife A 2204101 on January 17, 2013. The coordinates and name of the most recent station are used for the joined entire record.

B. Substituted Precipitation Data

For most airport staffed weather stations, part of the observing/reporting procedures include a suite of daily observations such as maximum and minimum temperatures and daily snow fall, rainfall, and total precipitation. At some staffed stations, however, arrangements are not in place with the Nav Canada staff or contractors for the daily observations. Examples include Regina, Winnipeg and Churchill stations which have not had staffed daily observations since 2007 or 2008. ECCC has co-located autostations with all-season weighing precipitation gauges providing daily total precipitation. These data are substituted for the absent staffed station precipitation data and used with the staffed station hourly data. Otherwise, these long-term stations with decades of icing event data would not be subject to updating.

The staffed station precipitation observations are made with a Nipher-shielded manual snow gauge and standard rain gauge. Weighing gauges at ECCC autostations generally are installed with a single Alter shield and are known to have a lower catch efficiency than the Nipher gauge owing to wind effects. The weighing gauge collection efficiency accounting for wind effects, CE , from [5] is:

$$CE = ae^{-bu} + c \quad (1)$$

where a , b and c are fitting coefficients and U is wind speed. For the single Alter weighing gauge, for mixed precipitation, and the wind speed (m/s) at 10 m above ground, the values of the coefficients are $a = 0.821$, $b = 0.077$, $c = 0.175$.

Since the precipitation during icing events is almost always mixed (liquid and frozen e.g. freezing rain, snow, ice pellets) the precipitation from these stations and years was adjusted for each hour by the reciprocal of CE in equation (1). Precipitation for the most recent periods of 13 stations was substituted in this manner.

C. Ice Accretion Models

The Châiné ice accretion model equation from [6] is:

$$\Delta R = -r + \left[r^2 + \frac{K r}{2} (t_h^2 + t_v^2)^{1/2} \right]^{1/2} \quad (2)$$

where ΔR is the incremental change in ice thickness (mm), r (mm) is the radius of the cylinder (conductor) at the start of the hour including ice already on the conductor, K is an adjustment factor (a function of temperature and the conductor radius), t_h is the hourly freezing precipitation (on a horizontal surface), and t_v is the hourly accretion on a vertical surface (mm) and is given by:

$$t_v = 1.231 V \left(\frac{P}{25.4} \right)^{0.88} \quad (3)$$

where V is the wind speed (km/h) and P is the freezing precipitation rate (mm/h). P is numerically the same value as t_h , the hourly freezing precipitation amount.

The correction factor from [6], based on wind tunnel icing results reported in [7], is adapted in a software routine from Fig. 1.

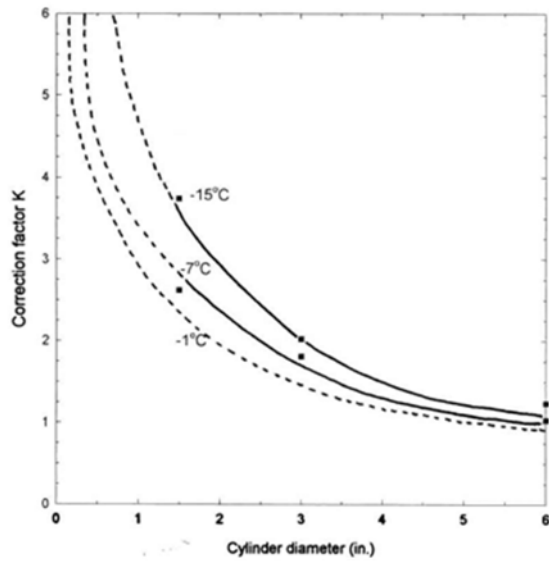


Fig. 1 Correction factor used with the Chaîné ice accretion model. The dashed lines indicate extrapolated values outside of the range of the original icing wind tunnel results.

Two other ice accretion models were implemented. Both the Goodwin and CRREL simple models assume that the freezing precipitation occurring each hour is intercepted by, and is distributed evenly around the conductor.

The Goodwin model equation after [8] is:

$$\Delta R = \frac{P}{\rho\pi} \sqrt{1 + \left(\frac{V_w}{V_t}\right)^2} \quad (4)$$

where ΔR is the incremental change in ice thickness (mm), P is the hourly freezing precipitation (mm), ρ is the specific gravity of ice (i.e. 0.9), V_w is the horizontal wind speed (m/s), and V_t is the terminal drop velocity (m/s).

The following expressions were used for V_t from [9]:

$$V_t = 201 (r_0/1000)^{-(1/2)} \quad \text{for } 0.6 < r_0 < 2.0 \text{ mm}$$

$$V_t = 8 r_0 \quad \text{for } r_0 < 0.6 \text{ mm} \quad (5)$$

where r_0 (m) is the median rain drop radius. The median drop diameter, d_0 (mm) is given by the following from [10], corresponding to the Marshall-Palmer drop size distribution:

$$d_0 = 3.67 / (4.1P^{0.21}) \quad (6)$$

where P (mm) is the hourly freezing precipitation amount.

The CRREL simple model equation from [11] is:

$$\Delta R = \frac{1}{\rho_i \pi} \sqrt{(P\rho_0)^2 + (3.6 V W)^2} \quad (7)$$

where ρ_i is the density of ice (0.9 g/cm³), ρ_0 (1 g/cm³) is the density of water, P is the freezing precipitation (mm), V is the wind speed (m/s), and W is the liquid water content (g/m³) of rain filled air given by the equation from [12]:

$$W = 0.067P^{0.846} \quad (8)$$

where P is hourly freezing rain amount in mm (numerically equivalent to rate in mm/h).

Reference [11] reports that the CRREL simple model (which is based on the Best drop size distribution) gives up to 9% less ice accretion than when using the Marshall-Palmer distribution, which provides a higher liquid water content than Best for a given precipitation rate (through a lower drop terminal fall speed). The Marshall-Palmer distribution

describes precipitation from stratiform cloud (not convective) which is generally more representative of freezing rain conditions. The implementation of the Goodwin and CRREL simple models for this project is consistent with differences noted in [11]. The Goodwin model results in consistently higher ice accretion amounts than the CRREL simple model. Also, the Chaîné model almost always results in higher event ice accretion amounts than either the Goodwin or CRREL simple models. This is well known and reported in many of the references, especially in [11] and [13].

D. Estimating Hourly Freezing Precipitation Amounts

All ice accretion models require estimates of the hourly freezing precipitation, which is provided by prorating the daily total precipitation amount for each precipitation type that occurs each hour, weighted by a nominal rate characteristic of each type and intensity observed.

The weights used for each precipitation type and intensity observed each hour is presented in Table 1.

TABLE I. WEIGHTS USED TO PRORATE THE DAILY TOTAL PRECIPITATION

Precipitation type/intensity	Light	Moderate	Heavy
R	1.8	5.1	13
RW	1.8	5.1	13
L	0.1	0.3	0.8
ZR	1.8	5.1	13
ZL	0.1	0.3	0.8
S	0.6	1.3	2.5
SG	0.6	1.3	2.5
IC	0	0	0
IP	1.8	5.1	13
IPW	1.8	5.1	13
SW	0.6	1.3	2.5
SP	0.6	1.3	2.5
A	1.8	5.1	13

The precipitation types are rain (R), rain shower (RW), drizzle (L), freezing rain (ZR), freezing drizzle (ZL), snow (S), snow grains (SG), ice crystals (IC), ice pellets (IP), ice pellet shower (IPW), snow shower (SW), snow pellets (SP) and hail (A).

The freezing precipitation each hour is determined by the sum of the ZR and ZL amounts from the weighting scheme.

E. Example of a Modelled Icing event

Fig. 2 presents an example of the evolution of a significant icing event at Sydney A, Nova Scotia beginning March 30, 2014 and lasting for more than 2 days. A number of characteristics of the ice accretion model results are evident. For the first 18 hours or so, the wind speed is lower than 20 km/h and the Goodwin and CRREL results are close but for the subsequent hours the wind speed increases and the Goodwin hourly accumulations are higher, reflecting the difference between the Goodwin's Marshall-Palmer drop size distribution and CRREL's Best distribution.

The Chaîné hourly accumulations at the start of the event are higher than either Goodwin or CRREL but decrease as the event progresses, reflecting lower values of the correction factor with increasing cylinder diameter. By the end of the event the Goodwin amount is higher than Chaîné. This only occurs for the most significant events. For almost all events, Chaîné has the highest amounts.

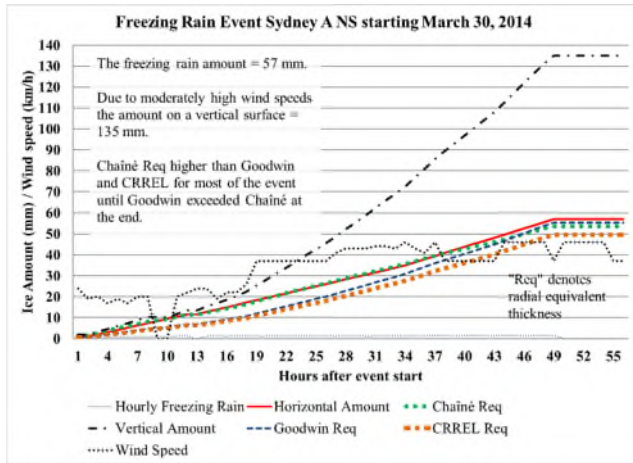


Fig. 2 Evolution of an Icing Event at Sydney A, Nova Scotia.

F. Comparison of the Chaîné Model with Observations

There are few regular, network observations of ice accretion due to freezing rain with which to compare ice accretion model results. Reference [14] describes a comparison of Chaîné model results with passive ice meter (PIM) observations from the provincial utility Hydro Quebec. The PIM observations are from manual measurements of ice accretion on 25 mm diameter cylinders situated 1.7 m above ground. The data set acquired from Hydro Quebec comprised the annual maximum ice thickness amounts for 235 locations for periods up to 16 years from 1974 to 1990. Twenty of the PIMs were at airport locations for which Chaîné model results were available. The Chaîné model was run using hourly wind speeds profiled with the log law from the 10 m standard height to 1.7 m above ground. The 30-year return period ice thickness was calculated from the Chaîné model for these 20 locations for data periods from 6 to 38 years using the Gumbel distribution fitted by the method of moments to the annual maximum series. The same approach was taken to calculate the 30-year PIM amounts at the same 20 locations. The average of the 30-year ice amounts was 12.35 mm (Chaîné) and 13.03 mm (PIM). The average difference was 1.11 mm and the standard deviation of differences was 5.47 mm. This was a very limited comparison, and although the average 30-year amount was similar, there was a large variation of the differences from location to location. One of the reasons for the large standard deviation is probably the differing data periods; nonetheless, there is a rough correspondence between the Chaîné model results and the PIM measurements.

Recent reference [15] reports results on an analysis of the ice-to-liquid ratio during freezing rain using observations in the United States from ASOS (Automated Surface Observing System) stations. The purpose was the development of a multivariable Freezing Rain Accumulation Model (FRAM) to assist the operational forecasting of ice accretion amounts on various objects and surfaces. Part of the work involved

calculating ice-to-liquid ratio of the ice accretion derived from the ASOS icing sensor (Goodrich Sensor System 827C3) and the total precipitation during freezing rain and then comparing with the CRREL simple model results. A conclusion presented is that the CRREL simple model tends to overestimate ice accretion in comparison with the observed data. By extension, this conclusion, to the degree that it corresponds to the manner in which the ice accretion models are applied in this project, can be assumed to apply to the Goodwin and Chaîné models too, the rough correspondence of Chaîné model results with Hydro Quebec PIM data reported in [14], notwithstanding.

A related issue concerns whether ice pellets contribute to the hourly freezing precipitation, and hence the modelled ice accretion results. As already described, for this project, the precipitation attributed to ice pellets is not included in the hourly freezing precipitation amount. In some applications (e.g. [16]), the water equivalent of ice pellets is included in the hourly freezing rain since ice pellets in this context is freezing rain that has frozen, and indicates that there might be freezing rain a short distance away either horizontally or at a higher height above ground. Reference [16] reports that the CRREL simple model ice accretion amount for the 1998 Ice Storm multi-day event at Mirabel A in southern Quebec was 54 mm. Of the hours with freezing rain, 48% included ice pellets, which were incorporated into the hourly freezing precipitation in [16]. In this project, the CRREL simple model result for this event was 35 mm. The assumption of including ice pellets as freezing precipitation often has a significant impact on the ice accretion amount.

G. Extreme Value Analysis (EVA) of the Icing Amounts

EVA is used to estimate the return period of a given event. Return period is the reciprocal of the annual exceedance probability. For example, the 50-year quantity such as the 50-year wind speed or ice thickness is the amount that has a 1/50 or 2% probability of occurring or being exceeded each year. The return period is also known as the recurrence interval since it is the average number of years between occurrences of events of that or greater magnitude. For Canadian standards the 50-year return level is a common reference level used for design purposes.

The application of EVA involves fitting an extreme value distribution to a selection of the extreme events from the observational record. For this project, the following combinations of distributions and methods were used to fit the annual maximum series of the ice accretion amounts.

- Gumbel 2-parameter distribution fitted by the method of moments [17] – GUM_MOM
- Gumbel 2-parameter distribution fitted by L-moments [18] – GUM_MLM
- Gumbel 2-parameter distribution fitted by generalized least squares [19] – GUM_GLS
- GEV (Generalized Extreme Value) 3-parameter distribution fitted by L-moments [18] – GEV_MLM (note that the GEV distribution reverts to the Gumbel when the 3rd parameter for shape tends to zero)



Fig. 3 Average annual number of discrete icing events (top number) and annual average number of hours of freezing precipitation (bottom number) for each Canadian province and territory.

EVA has a theoretical basis with certain assumptions, such as the block of data from which maxima are selected being comprised of many independent events. For some observations such as wind speed, this is often the case, but for icing events this can be problematic owing to only a few events each year. For instance, Fig. 2 shows for each Canadian province and territory, the annual average number of icing events and the annual average number of hours of freezing precipitation generated from the results of this project. The average number of icing events range from 1 per year on the west coast to 10 on the east coast – not enough to satisfy the requirements of EVA theory. Nonetheless, the EVA distributions are commonly used for this purpose, on the basis of reasonable fits to the data. In particular, the Gumbel distribution fitted by the method of moments is the approach used in the analysis of results for this project.

H. Accounting for Non-Icing years

A further issue arises since there are several locations with years of complete observations, but experiencing no icing events. Some coastal BC locations have more non-icing years than icing years. For instance, Spring Island, on the west coast of Vancouver Island in BC, experienced three icing events in a period of 26 years. Rather than include the non-icing years with icing years in the AMS for an EVA analysis, they are treated as a separate population and their probability of occurrence (zero) is combined with the EVA analysis in calculating the return level of icing thickness by the following approach.

The return period to result in an overall equivalent return period of 50 years, accounting for the non-icing years, T_{50eq} , is:

$$T_{50eq} = 50 \, n_{ice} / n_{tot} \quad (9)$$

where n_{ice} is the number of non-icing years in the period of n_{tot} years that includes icing years. EVA is applied to the non-zero AMS members and the return level of T_{50eq} is used instead of 50, to calculate the equivalent 50-year return level that accounts for non-icing years. Fig. 4 shows an EVA graph for Abbotsford A, BC, for the radial ice thickness on a 25 mm diameter conductor.

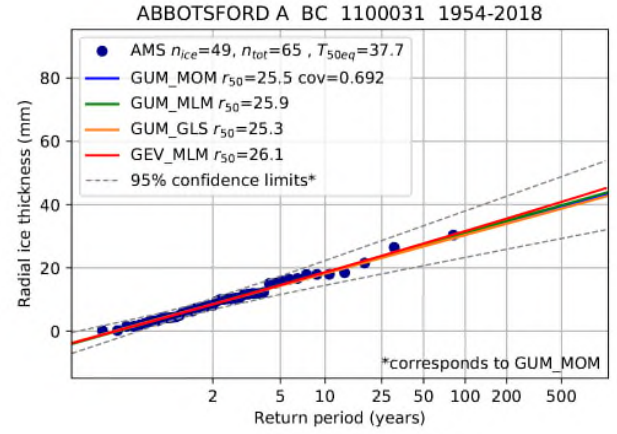


Fig. 4 EVA graph with four distribution/fitting combinations. r_{50} is the 50-year return level radial ice thickness (mm), after accounting for non-icing years. cov (coefficient of variation) is the standard deviation of the AMS (icing years) divided by its mean. Refer to the text for descriptions of other terms.

Note that the EVA method using peak-over-threshold extremes analysed with the Generalized Pareto Distribution automatically accounts for non-icing years.

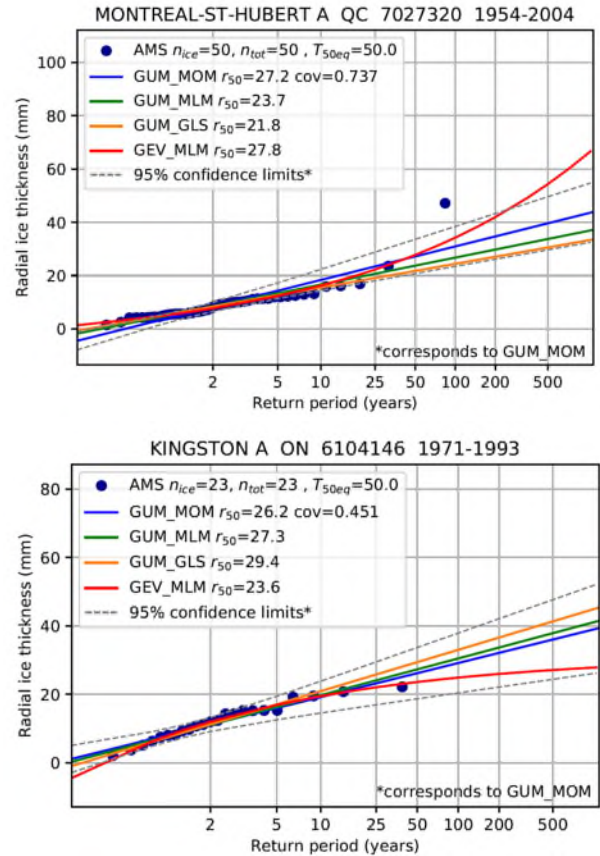


Fig. 5 EVA graph with four distribution/fitting combinations. St-Hubert (top) is an example of a GEV fit with a negative shape factor. Kingston (bottom) has a positive shape factor. Refer to Fig. 4 caption for descriptions of terms.

I. Examples of EVA Results

The purpose of four distribution/fitting methods in this project was to allow comparison between results. In Fig. 4, the AMS members all fit well on the double-log scale Gumbel x-axis. There is little difference in the return level results

amongst the four methods. Note that the three Gumbel fits will always be a straight line, and the 3-parameter GEV fit may curve, depending on the value of its shape parameter. If the shape parameter approaches zero, the GEV fit approaches a Gumbel distribution and hence a straight line.

Fig. 5 illustrates examples for which the four methods show differences. The Montreal-St-Hubert fit reflects a GEV negative shape factor, and Kingston A, a positive shape factor with upward and downward curving GEV fits, respectively. For the 215 station EVA results, a negative GEV shape factor is more common than a positive value. The GEV fit provides the most conservative result for 50-year return levels and higher. The GUM_MOM fit provides the next most conservative (or conversely, the second least conservative result for positive GEV shape factors). Although these differences are interesting, and always a source of discussion amongst analysts, for this project, the GUM_MOM results were used for further analysis.

III. RESULTS

Results comprising the 50-year return levels of radial thickness on a 25 mm conductor, ice thickness on a horizontal surface and ice thickness on a vertical surface were compiled for 215 stations with at least 10 years data over the period of winter years 1954-2018. The locations are presented in Fig. 6. All represent staffed weather stations almost all at airports with the present weather and manual daily total precipitation observations required for the ice accretion modelling aspects of the project. Thirteen used substituted, wind-adjusted, all-weather single Alter-shielded weighing gauge daily total precipitation for some years at the ends of their periods.



Fig. 6 Locations of 215 staffed weather stations used to generate the ice accretion results for this project.

A. Results for Radial Ice Thickness on a Conductor

The standards for transmission lines and telecommunication towers specify reference ice thickness as the 50-year return level of radial thickness on a 25 mm conductor. The 50-year radial thickness amounts resulting from the Gumbel method of moments fit (GUM_MOM) to the AMS for each of the 215 stations were used to compile a contour map illustrating the spatial pattern of values as illustrated in Fig. 7. The individual station values were plotted on screen using GIS software and the contours placed using the judgement of the analyst.

The most prominent feature of the map is that the highest amounts are in eastern Canada, reflecting the higher frequency of freezing rain illustrated in Fig. 3. The highest values (40 mm) occur over eastern Newfoundland. In Atlantic Canada, values higher than 30 mm occur over Prince Edward Island, the southern shore of Newfoundland, and eastern New Brunswick and Nova Scotia. Values higher than 30 mm also occur in the icing-prone areas of the St. Lawrence and Ottawa valleys in south western Quebec and eastern Ontario, and along the north shore of Lake Erie in south western Ontario. Most of western Canada is less than 10 mm. However, there is a higher zone of greater than 20 mm along the western shore of Hudson Bay. Coastal BC has higher values than 15 mm in the mainland coastal inlets and valleys where moist Pacific air overruns cold interior air outflowing through coastal valleys. The map reflects this feature and locally some stations such as Abbotsford A and Terrace A indicate values higher than 20 mm.

In some areas, especially in western Canada, it is recognized that the governing ice loads are not due to freezing rain. For example, the provincial regulator in Alberta specifies ice loading zones due to frozen wet snow in [20]. Standard [2] accommodates this with supplementary frozen snow accretion amounts for Alberta consistent with [20] that are significantly higher than the ice accretion amounts due to freezing rain.

These updated values reflect an additional ten years of data since the previous update conducted with data up to 2007, so are generally similar to existing maps in the CSA standards. The results of this project will be made available to CSA technical committees for consideration of updating the standards.

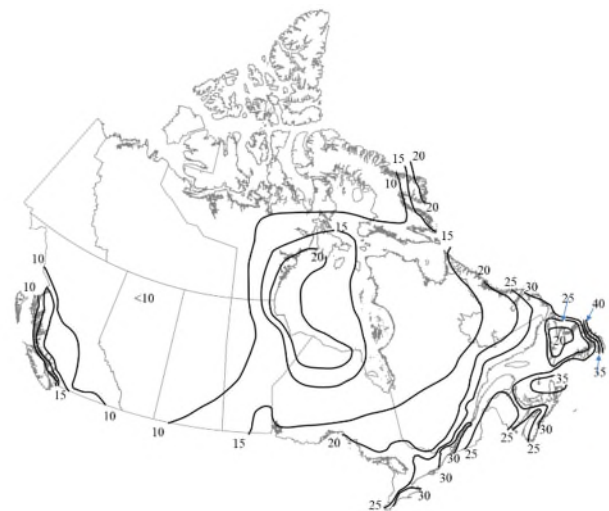


Fig. 7 50-year radial ice thickness values (mm) on a 25 mm conductor.

B. Results for Ice Thickness on Flat Surfaces

Standard [4] ice amounts for highway bridge design specifies the 50-year return level ice thickness on a flat (vertical or horizontal) surface, whichever is greatest. From the EVA results for the 215 stations in this project, the value at each point (greatest of the 50-year amounts on a vertical or horizontal surface) was plotted onscreen and the ice zones in Fig. 8 determined using the judgment of the analyst. The ice zone definitions are similar to those already in the standard [4]. The map in the current standard was developed in the 1970's

using a similar approach except that length of the data sets available as input for the Chaîné ice accretion model at that time was from 9 to 15 years. There were a few other changes in the analysis but general pattern in Fig. 8 is similar with some variation in local details. These values generally reflect the ice on a vertical surface, owing to moderate or higher wind speeds during an icing event, rather than the lower horizontal surface amounts. This effect is evident in Fig. 2, the icing event example from Sydney A. The radial thickness for the event is 55 mm, the amount on a horizontal surface is 57 mm and the amount on a vertical surface is 135 mm.

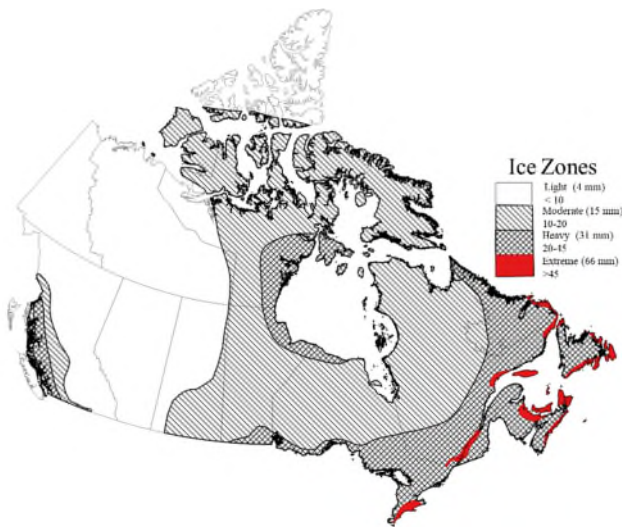


Fig. 8 Ice zones based on 50-year ice thickness values (mm) on a flat vertical or horizontal surface, whichever is greatest. The nominal values and range of each zone is indicated in the legend.

IV. EFFECTS OF A CHANGING CLIMATE ON ICE ACCRETION

Climate change effects on structural loads is a subject of increasingly high interest in the codes and standards community. A primary point of concern is the probability of loads changing (increasing, especially) in the future compared to those determined in the traditional manner of analysing the recent climate record (such as was done for this project), and assuming the result represents the future, at least for the lifetime of structures being designed. One such recent study [21] investigated the effects of climate change specifically on extreme (50-year return level) ice accretion amounts due to freezing rain in North America.

The general approach was to use a large 50-member initial-condition ensemble of the CanRCM4 regional climate model, driven by CanESM2 general climate model under the RCP8.5 high emissions (business-as-usual) scenario to simulate a baseline period 1986-2016 and four 31-year future periods ending in 2053-2083. The CanRCM4 model results at 0.44° spatial resolution and 3-hourly time steps at the surface and three upper levels (500, 850 and 1000 hPa) were used to calculate freezing precipitation at the surface. The Chaîné ice accretion model was used to calculate 50-year return level radial and vertical and horizontal surface amounts by fitting the Gumbel distribution. The changes for each grid point were calculated for each future period relative to the baseline period, for each grid point, and for each of the 50 ensemble members. Results were presented for the ensemble average and the 5th

and 95th percentile ensemble value in the form of maps over North America, an excerpt of which is presented in Fig. 9.

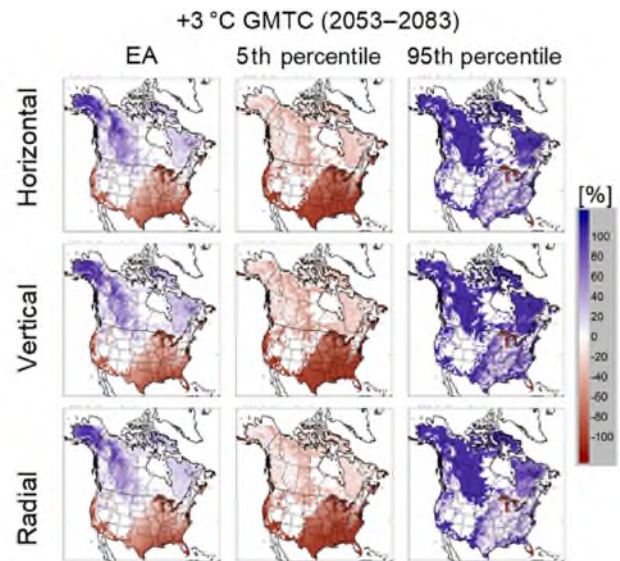


Fig. 9 Changes (%) in the 50-year return level radial, vertical and horizontal ice accretion amounts for the ensemble average (EA) and 5th and 95th percentile ensemble result, corresponding to the period 2053-2083, compared to the base period 1986-2016. This period represents a 3°C global mean temperature change (GMTC) under the RCP8.5 emissions scenario. From [21].

The results in Fig. 9 represent the greatest degree of change, since it is the period farthest into the future that was simulated. The EA results for all the fields show decreases south of about 40°N and increases to the north, except decreases in the southern Atlantic Provinces. It is notable that all of the 5th percentile ensemble results show decreases everywhere and the 95th percentile results show increases everywhere (except the Great Lakes). The variation across the ensemble members indicates qualitatively a moderate degree of confidence in the EA change values. The EA results show that percentage increases are generally highest where the current amounts are lowest (across western and northern Canada), except for the upper St. Lawrence valley in Quebec. Conversely, for the other areas of high amounts e.g. southern Ontario and the Atlantic provinces, decreases are indicated. The authors of [21] note the substantial increases north of 40°N have clear implications for future building and infrastructure design. Results such as these add an additional dimension to the work of the structural standards community and is likely to be a source of lively discussion.

V. CONCLUSIONS

Design ice accretion amounts due to freezing rain for Canadian codes and standards were updated using data from 215 airport weather stations with periods of record ranging from 10 to 65 years from the period 1954-2018. Maps and related information of 50-year return level radial thickness around a 25 mm conductor and on flat vertical and horizontal surfaces were prepared and are available for updating Canadian standards for overhead electrical transmission lines, telecommunication towers and highway bridge design. A recent investigation of the impact of climate change on the design ice amounts is referenced and discussed. These results

indicate that for much of Canada, significant increases of the design ice amounts are projected.

ACKNOWLEDGMENT

This work was supported by funding from the National Research Council of Canada-led project on Climate-Resistant Buildings and Core Public Infrastructure under the Pan-Canadian Framework on Clean Growth and Climate Change.

REFERENCES

- [1] *Overhead Systems*, CAN/CSA-C22.3#1-15, 2015.
- [2] *Design Criteria of Overhead Transmission Lines*, CAN/CSA-C22.3#60826-10, 2010.
- [3] *Towers, Antennas and Antenna-Supporting Structures*, CAN/CSA-S37-18, 2018.
- [4] *Canadian Highway Design Bridge Code*, CAN/CSA-S6-14, 2014.
- [5] John Kochendorfer, Rodica Nitu, Mareile Wolff, Eva Mekis, Roy Rasmussen, Bruce Baker, Michael E. Earle, Audrey Reverdin, Kai Wong, Craig D. Smith, Daqing Yang, Yves-Alain Roulet, Samuel Buisan, Timo Laine, Gyuwon Lee, Jose Luis C. Aceituno, Javier Alastrué, Ketil Isaksen, Tilden Meyers, Ragnar Brækkan, Scott Landolt, Al Jachcik, and Antti Poikonen, "Analysis of single-Alter-shielded and unshielded measurements of mixed and solid precipitation from WMO-SPICE", *Hydrol. Earth Syst. Sci.*, vol. 21, pp. 3525–3542, 2017. <https://doi.org/10.5194/hess-21-3525-2017>.
- [6] P. M. Chaîné and G. Castonguay. "New approach to radial ice thickness concept applied to bundle-like conductors", Environment Canada, Toronto, ON, Industrial Meteorology-Study IV, 1974.
- [7] J. R. Stallabrass and P.F. Hearty, "The icing of cylinders in conditions of simulated sea spray", National Research Council of Canada, Ottawa, ON, Mechanical Engineering Report MD-50, 1967.
- [8] E. J. Goodwin, J. D. Mozer, A. M. DiGioia, and B. A. Power, "Predicting Ice and Snow Loads for Transmission Line Design", *Proceedings of the First International Workshop on Atmospheric Icing of Structures*, Hanover, NH, 1981.
- [9] R. R. Rogers, and M. K. Yau. *A Short Course in Cloud Physics*, 3rd ed., (page 126), Butterworth-Heinemann, Woburn, MA, 1989.
- [10] D. Atlas, R. C. Srivastava, and R. S. Sekhon, "Doppler Radar Characteristics of Precipitation at Vertical Incidence", *Reviews of Geophysics and Space Science*, vol. 849, p.p. 1-34, 1973.
- [11] K. F. Jones, "A simple model for freezing rain ice loads", *Atmospheric Research*, vol. 46, pp. 87- 97, 1998.
- [12] A. C. Best, "The size distribution of raindrops", *Q. J. Royal Met. Soc.*, vol. 75, pp. 16-36, 1949.
- [13] K. F. Jones and R. Morris, "Investigation of the Differences in the Application of the Canadian and U.S. Methodology for Estimates of Ice Loads for a 50-yr Return Period", CEATI, Montreal, QC, Report No.T003700-3306, 2002.
- [14] T.-C. Yip, "Estimating icing amounts caused by freezing precipitation in Canada", *Atmospheric Research*, vol. 36, pp. 221- 232, 1995.
- [15] Kristopher J. Sanders and Brian L. Barjenbruck, "Analysis of Ice-to-Liquid Ratios during Freezing Rain and the Development of an Ice Accumulation Model", *Weather and Forecasting*, vol. 31, pp. 1041-1060, August, 2016. DOI: 10.1175/WAF-D-15-0118.1.
- [16] K. F. Jones, "Ice Storms in the St. Lawrence Valley Region", Cold Regions Research and Engineering Laboratory, Report ERDC/CRREL TR-03-1. 2003.
- [17] M. D. Lowery and J. E. Nash, "A Comparison of Methods of Fitting the Double Exponential Distribution", *Journal of Hydrology*, vol. 10, pp. 259-275, No. 3, 1970.
- [18] Hosking, J.R.M. and J.R. Wallis. *Regional Frequency Analysis. An Approach Based on L-moments*. Cambridge University Press, Cambridge, UK, 1997.
- [19] H. P. Hong, S. H. Li, and T. G. Mara, "Performance of the generalized least-squares method for the Gumbel distribution and its application to annual maximum wind speeds", *Journal of Wind Engineering and Industrial Aerodynamics*, vol. 119, pp. 121-132, 2013.
- [20] (2010) The Alberta Electrical System Operator website. [Online]. Available: <https://www.aeso.ca/assets/downloads/2011-08-12-Wet-Snow-And-Wind-Loading-Map.pdf>
- [21] Dae Il Jeong, Alex J. Cannon, and Xuebin Zhang, "Projected changes to extreme freezing precipitation and design ice loads over North America based on a large ensemble of Canadian regional climate model simulations", *Nat. Hazards Earth Syst. Sci.*, vol. 19, pp. 857–872, 2019. <https://doi.org/10.5194/nhess-19-857-2019>.